Radiating Instability of a Meridional Boundary Current

HRISTINA G. HRISTOVA

MIT–WHOI Joint Program in Oceanography, Woods Hole, Massachusetts

JOSEPH PEDLOSKY AND MICHAEL A. SPALL

Woods Hole Oceanographic Institution, Woods Hole, Massachusetts

(Manuscript received 7 June 2007, in final form 1 February 2008)

ABSTRACT

A linear stability analysis of a meridional boundary current on the beta plane is presented. The boundary current is idealized as a constant-speed meridional jet adjacent to a semi-infinite motionless far field. The far-field region can be situated either on the eastern or the western side of the jet, representing a western or an eastern boundary current, respectively. It is found that when unstable, the meridional boundary current generates temporally growing propagating waves that transport energy away from the locally unstable region toward the neutral far field. This is the so-called radiating instability and is found in both barotropic and two-layer baroclinic configurations. A second but important conclusion concerns the differences in the stability properties of eastern and western boundary currents. An eastern boundary current supports a greater number of radiating modes over a wider range of meridional wavenumbers. It generates waves with amplitude envelopes that decay slowly with distance from the current. The radiating waves tend to have an asymmetrical horizontal structure—they are much longer in the zonal direction than in the meridional, a consequence of which is that unstable eastern boundary currents, unlike western boundary currents, have the potential to act as a source of zonal jets for the interior of the ocean.

1. Introduction

Radiating instability refers to an instability of the mean flow that propagates energy away from the source of instability. It can be contrasted with a trapped instability, the influence of which is confined mainly to the locally unstable region and has no impact on the far field. Previous studies have shown that parallel zonal eastward barotropic jets do not support radiating instabilities (Talley 1983). For these currents, the perturbation energy stays trapped near the mean jet and none is radiated toward the far field. However, radiating instabilities are possible if the far field is made baroclinic or if a westward component is added to the jet (Talley 1983). Another way to obtain radiation is by introducing even slight nonzonality in the mean flow (Kamenkovich and Pedlosky 1996).

A meridional current can be seen as an extreme case of nonzonality. The stability of meridional currents is less studied in the literature but is nonetheless of great interest. Because of the presence of continents, boundary currents that are meridional or close to meridional are present on both sides of most ocean basins. Unstable boundary currents can be an important source of eddy kinetic energy. If the instabilities are radiating, then the energy of the disturbances will be transported long distances and will be able to potentially affect the mean circulation and its variability in the interior of the basin. Radiating instabilities propagate energy away from the locally unstable region by coupling to the free Rossby waves in the far field. This brings attention to a possible difference between eastern and western boundary currents. Because short and long Rossby waves have different zonal directions of propagation, it introduces an asymmetry between eastern and western boundary currents. One could expect, therefore, different radiating properties depending on which side of the basin the current is situated on.

There are several previous studies relevant to the stability of meridional flows. In Walker and Pedlosky (2002), attention is paid to the baroclinic instability of a

Corresponding author address: Hristina Hristova, Woods Hole Oceanographic Institution, Clark MS#21, Woods Hole, MA 02543.
E-mail: hhristova@whoi.edu

DOI: 10.1175/2008JPO3853.1

© 2008 American Meteorological Society

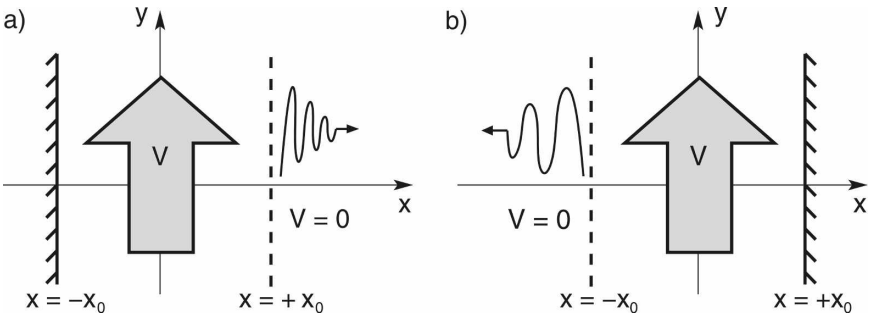

FIG. 1. Basic state for the stability problem. Configurations for (a) a western and (b) an eastern boundary current.

two-layer meridional flow in a channel. Compared to its zonal counterpart, the main distinction is that an arbitrarily small vertical shear leads to growing perturbations. The lack of critical threshold for linear stability is a consequence of the fact that the contributions to the mean potential vorticity gradient coming from the planetary vorticity and the mean shear are in different directions. Meridional currents are also known to have radiating instabilities. In Fantini and Tung (1987), the particular case of a meridional barotropic boundary current situated on the western side of a basin and adjacent to a motionless, semi-infinite region is addressed. The authors find that radiating unstable waves are generated, which propagate energy eastward toward the ocean interior. The unstable waves have long meridional wavelengths and phase speeds that are larger than those of the jet that generates them.

The objective here is to expand our knowledge of radiating instabilities of meridional boundary currents. This is done in the context of a layered quasigeostrophic (QG) model on the β plane with no dissipation. As in Fantini and Tung (1987), the boundary current is idealized by a piecewise constant profile bounded by a solid wall on one side and a semi-infinite motionless far-field region on the other side. By solving the resulting linear stability problem, one can find whether and under what conditions the meridional current can have radiating instabilities. Compared to previous studies, emphasis is placed on the differences between the stability properties of eastern and western boundary currents. Also, both barotropic and two-layer baroclinic configurations are studied.

The plan of the presentation is as follows: section 2 presents the formulation of the problem and discusses the results for the barotropic QG model. It also gives some extended discussion on the structure of the radiating instabilities. Section 3 deals with the stability of a purely baroclinic meridional current using a two-layer QG model. Some final conclusions and physical implications are given in section 4.

2. The barotropic case

a. Formulation

For reasons of mathematical convenience, the boundary current is idealized as the piecewise constant meridional velocity profile

$$V = \begin{cases} V_*, & |x| < x_0 \\ 0, & |x| > x_0 \end{cases}, \tag{1}$$

as in Fantini and Tung (1987). The velocity V_* is taken positive without loss of generality. Depending on where the motionless far field is located, the flow corresponds to a western or an eastern boundary current as shown in Fig. 1. The basic state is sustained by some large-scale forcing, not specified here because it does not appear in the linear stability problem. The departures $\psi(x, y, t)$ from the basic state are decomposed into normal modes:

$$\psi(x, y, t) = \mathrm{Re}[\phi(x)e^{im(y-ct)}], \tag{2}$$

where m is the meridional (downstream) wavenumber and c is the phase speed in that direction. The amplitude $\phi(x)$ satisfies the linearized barotropic quasigeostrophic potential vorticity equation

$$(V - c)(\phi'' - m^2\phi) + \frac{\overline{Q}_y}{im}\phi' - \overline{Q}_x\phi = 0, \tag{3}$$

where $(\overline{Q}_x, \overline{Q}_y)$ is the potential vorticity gradient of the basic state given by

$$\overline{Q}_x = \frac{d^2V}{dx^2}, \quad \overline{Q}_y = \beta. \tag{4}$$

All variables above are nondimensionalized using as scales the current width $L_* = 2x_0$ and the current velocity V_*. The nondimensional planetary vorticity gradient is $\beta = \beta_0 L_*^2/V_*$.

For the basic state chosen here, Eq. (3) can be further simplified because the horizontal shear and $\overline{Q}_x$ are identically zero. Special care has to be taken, however,

of the points $x = \pm x_0$, where the velocity V is discontinuous. At these points, jump conditions derived from Eq. (3) hold (Kamenkovich and Pedlosky 1996). Their role is to impose the continuity of the streamline slopes and the tangential pressure gradient

$$\Delta\left[\frac{\phi}{V-c}\right] = 0, \quad \Delta\left[(V-c)\phi' + \frac{\beta}{im}\phi\right] = 0. \quad (5)$$

Here, $\Delta[\,\cdot\,]$ indicates the jump of the quantities in the brackets at the point $x = +x_0$ for a western boundary current and $x = -x_0$ for an eastern boundary current. The boundary condition on the other side of the current, where there is a solid wall, is $\phi = 0$ (i.e., no-normal flow).

The advantage of choosing a piecewise constant basic flow is that the stability problem (3) becomes a constant coefficient ODE. The amplitude ϕ is thus of the form $\phi \sim Ae^{ikx}$, where the zonal wavenumber k is related to the phase speed c, the meridional wavenumber m, and the other parameters of the problem through a dispersion relation. What is left is to impose the boundary and jump conditions at $x = \pm x_0$, which leads to a homogeneous algebraic system. The eigenvalues c are found by solving numerically the nonlinear equation that results from requiring the determinant of the homogeneous system to be zero so that there is a nontrivial solution. Once the eigenvalues c are found, the solution in both the far field and the boundary current region can be reconstructed. More details on the method of solution are given in the appendix.

b. Identifying the radiating instabilities

Suppose that for a given parameter β and a meridional wavenumber m we have found a value for the phase speed c such that the stability problem (3) as well as all boundary and jump conditions are satisfied. In the far-field region ($|x| > x_0$), the solution is then of the form

$$\psi(x, y, t) = \mathrm{Re}[Ae^{ik_r x}e^{im(y-c_r t)}]e^{-k_i x}e^{mc_i t}, \quad (6)$$

where the zonal wavenumber k is related to the frequency $\omega = cm$ (in general, a complex number) through the barotropic Rossby wave dispersion relation

$$cm = -\frac{\beta k}{k^2 + m^2}. \quad (7)$$

The solution (6) consists of a wave with amplitude envelope that for unstable modes ($mc_i > 0$) is growing in time and decaying with distance from the source. The spatial decay is a consequence of the fact that for a perturbation growing in time *and* propagating, the amplitude observed far from the source has been generated at an earlier time and is thus smaller than what is currently observed near the source. From (7) it follows that for each eigenvalue c, there are two solutions for the zonal wavenumber k. As shown in Fantini and Tung (1987), these two solutions have opposite-signed imaginary parts k_i as well as zonal group velocities. One of these solutions is appropriate for a western boundary current and the other for an eastern boundary current, because the two configurations require different sign k_i to have vanishing perturbation at infinity [see (6)]. Equivalently, one can say that given the eigenvalue c, the far-field solution consists only of the Rossby wave that has zonal group velocity away from the locally unstable region.

Because a radiating unstable solution decays into the far field very much as it is expected from a trapped one, it may be confusing at first how to distinguish between the two. The distinction, however, is clear in the weakly unstable limit. In the limit $c_i \to 0$, the far-field structure of a radiating solution becomes a pure Rossby wave (i.e., $k_i \to 0$), while for a trapped solution k_i stays finite. A mathematical expression of the statement above can be obtained from expanding the complex Rossby dispersion relation (7) in a Taylor series where k_i is the small parameter (i.e., $k = k_r + ik_i$ and $|k_i| \ll |k_r|$). If only the first-order term in k_i is kept, we obtain for the eigenvalue

$$c(k_r + ik_i) = c(k_i = 0) + ik_i\frac{\partial c}{\partial k}(k_i = 0) + O(k_i^2). \quad (8)$$

The real part of (8) states that

$$c_r \approx c(k_i = 0) = -\frac{\beta k_r}{m(k_r^2 + m^2)}. \quad (9)$$

In other words, in this limit the *real parts* of the eigenvalue c and the zonal wavenumber k are related through the Rossby dispersion relation. In particular, for given β and m, there is a real-valued solution for k_r only if the phase speed c_r lies within the allowable range for barotropic Rossby wave phase speeds, which is $-\beta/2m^2 < c_r < \beta/2m^2$. For meridional phase speed c_r that satisfies this condition, there are two possible values for k_r that correspond to a zonally long ($k_r < m$) and zonally short ($k_r > m$) wave and are solutions for an eastern and a western boundary current, respectively. If c_r does not satisfy the condition above, then k_r is actually complex and the solution in the far field is exponentially decaying, not a radiating wave.

The imaginary part of (8) states that

$$c_i \approx k_i\frac{\partial c}{\partial k}(k_i = 0) = \frac{k_i}{m}c_g^x(k_i = 0), \quad (10)$$

where $c_g^x = \beta(k_r^2 - m^2)/(k_r^2 + m^2)^2$ is the zonal group velocity of free barotropic Rossby waves. It follows that the spatial decay scale in the far-field $1/k_i$ is propor-

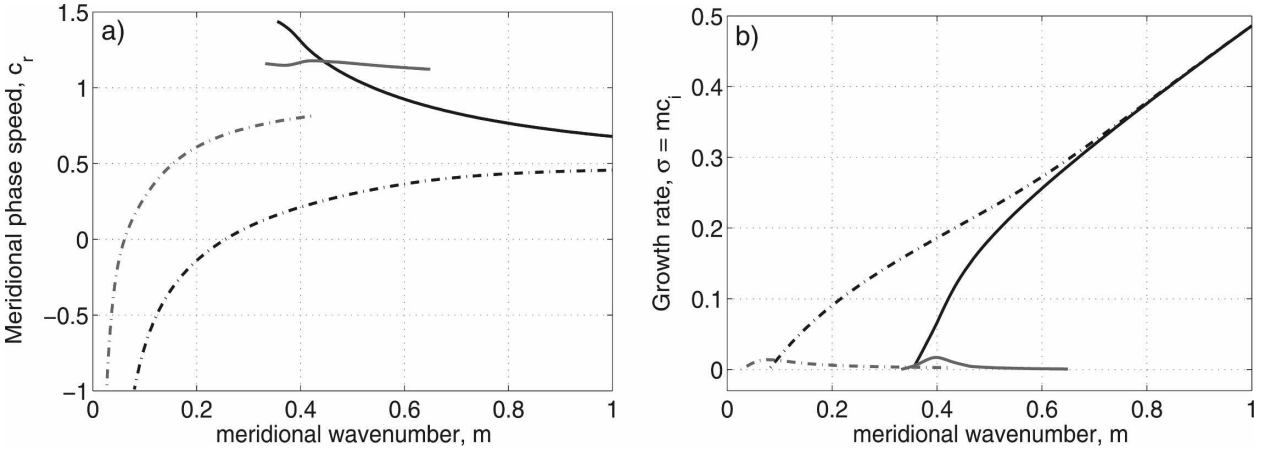

FIG. 2. (a) Meridional phase speed and (b) growth rate as a function of the meridional wavenumber for the barotropic case with $\beta = 0.5$. Solid lines are used for the western boundary current and dotted–dashed lines for the eastern boundary current. For each configuration, the most unstable eigenvalue is shown in black and the next unstable eigenvalue in gray.

tional to the group velocity c_g^x and the inverse of the growth rate mc_i. Thus, radiating unstable waves have amplitude envelopes that decay away from the source because packages of bigger and bigger amplitude are propagated at c_g^x as time advances.

For practical purposes, to determine if an eigenmode corresponds to a radiating instability, one follows the unstable mode until it becomes marginally stable (i.e., $c_i = 0$). If k_i also vanishes in this limit, then the instability is radiating. The mode has a radiating wave structure in the far field roughly as long as $0 < |k_i| < |k_r|$ (Fantini and Tung 1987; Kamenkovich and Pedlosky 1996).

c. Results

The only nondimensional parameter that characterizes the barotropic problem is the β parameter, defined previously as $\beta = \beta_0 L_*^2/V_*$, where L_* and V_* are the current width and velocity, respectively. The linear stability problem defined in section 2a is solved for the specific choice $\beta = 0.5$, a typical order one value, but the results are qualitatively representative of the general behavior of the system. When solving the eigenvalue problem, we are interested in finding the unstable eigenvalues and following them as the meridional wavenumber m is varied so that we can determine whether they are radiating or not.

1) WESTERN BOUNDARY CURRENT

The results are in essence the same as in Fantini and Tung (1987), except for the different choice of β. In the short-wave end of the explored range of meridional wavenumbers, there is a single unstable eigenvalue (solid black line in Fig. 2) that asymptotes to $c = 0.5 + i0.5$ when $m \to +\infty$. The lack of short meridional wave cutoff is artificial and is due to the choice of discontinuous basic-state profile. When the meridional wavenumber m is decreased, the growth rate mc_i for this mode decreases and reaches zero at $m_* = 0.355$ while its meridional phase speed c_r increases and eventually becomes larger than one (i.e., faster than the current). Besides this mode, an additional number of unstable eigenvalues, not mentioned in Fantini and Tung (1987), are found (a representative is shown in Fig. 2 with a solid gray line). All these modes have $c_r > 1$; that is, they are faster than the current (see Fig. 2a). Because of the trend of c_i to decrease to zero while c_r goes to 1 when the meridional wavenumber is increased, they are thought to originate in their short-wave limit from the singular point $c = 1$. Because of the singularity, however, the point $c = 1$ cannot be reached numerically and this is only assumed. Their growth rates are significantly weaker, but they exist for slightly smaller values of $m < m_*$ (see Fig. 2b). Nevertheless, as concluded in Fantini and Tung (1987), it is found that there is a long meridional wave cutoff for the linear stability of a western boundary current. Hence, for meridional wavenumbers below the cutoff value, all eigenvalues have negative imaginary parts (i.e., the current is linearly stable).

Concerning the radiating nature of the instabilities, it is the long-wave end of the explored range of meridional wavenumbers, when $c_r > 1$, that qualifies as radiating. In Fig. 3a the logarithm of the ratio $|k_r|/|k_i|$, k_r, and k_i being the real and imaginary part of the zonal wavenumber in the far field, is plotted as a function of m. For all modes, when the meridional wavenumber is decreased, the ratio $|k_r|/|k_i|$ goes to infinity while the

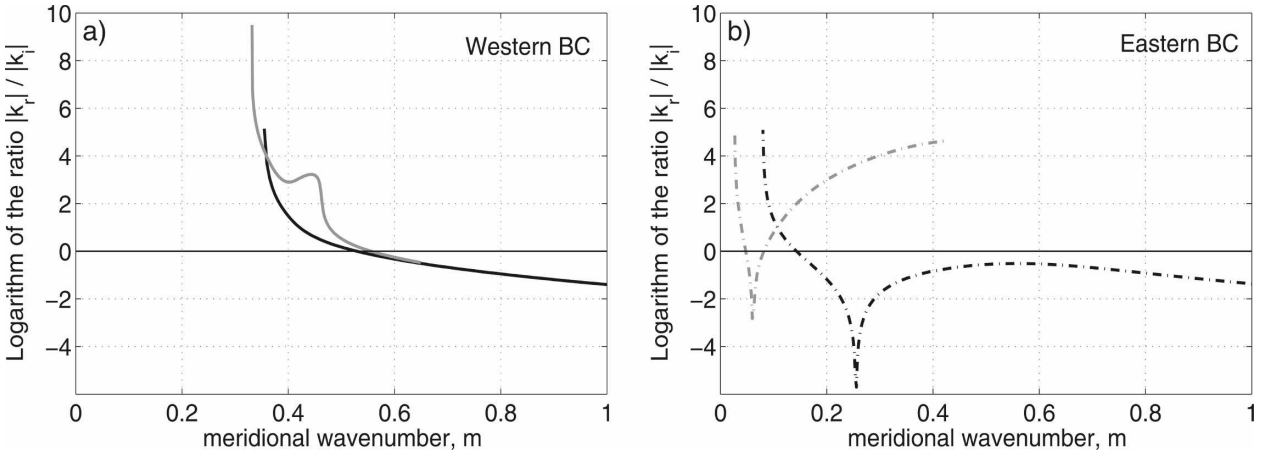

FIG. 3. Logarithm of the ratio $|k_r|/|k_i|$ as a function of the meridional wavenumber for the barotropic case for the (a) western and (b) eastern configurations. Here, k_r and k_i are the real and imaginary parts, respectively, of the zonal wavenumber in the far field. Line and black–gray code as in Fig. 2. Positive values indicate radiating wave structure.

growth rate decreases, which indicates that in the limit of zero growth rate the solution is a pure wave ($k_i = 0$). The modes have a radiating wave structure, defined by $|k_r| > |k_i|$ or positive values for $\log(|k_r|/|k_i|)$, over some interval of meridional wavenumbers before they stabilize. The structure of the eigenmodes in the far field depends strongly on the meridional wavenumber and the growth rate. In general, the weaker the growth rate, the shorter in the zonal direction are the radiated waves and the larger is the amplitude envelope decay scale. In Fig. 4 a typical example of a far-field solution is shown. The radiating wave has a meridional wavelength of $2\pi/m \approx 18$ current widths, a zonal wavelength of $2\pi/k_r \approx 5$ current widths, and an envelope decay scale of $1/k_i \approx 90$ current widths. For example, if the parameter $\beta = 0.5$ is representative of a 100-km wide current with speed 40 cms^{-1}, then the radiated wave has a zonal wavelength of 500 km, an envelope decay scale of 9000 km, and a growth rate of approximately (2.5 yr)$^{-1}$.

2) EASTERN BOUNDARY CURRENT

To satisfy the condition of a vanishing perturbation at infinity, a western boundary current selects solutions in the far field that have positive zonal group velocity, while for an eastern boundary current the solutions have negative zonal group velocity. This difference has a strong effect on the stability properties of the current.

The short-wave end of the explored range of meridional wavenumbers is similar for the western and eastern configurations. There is a single unstable eigenvalue (dotted–dashed black line in Fig. 2) that asymptotes to $c = 0.5 + i0.5$ when $m \to +\infty$. Looking back at Eq. (3), one can see that in this limit the term β/im responsible for the asymmetries in the propagation properties between east and west is not important. When the meridional wavenumber is decreased, however, differences appear. The meridional phase speed c_r of the mode decreases, unlike for the western boundary current case. When the mode finally stabilizes at $m_* =$

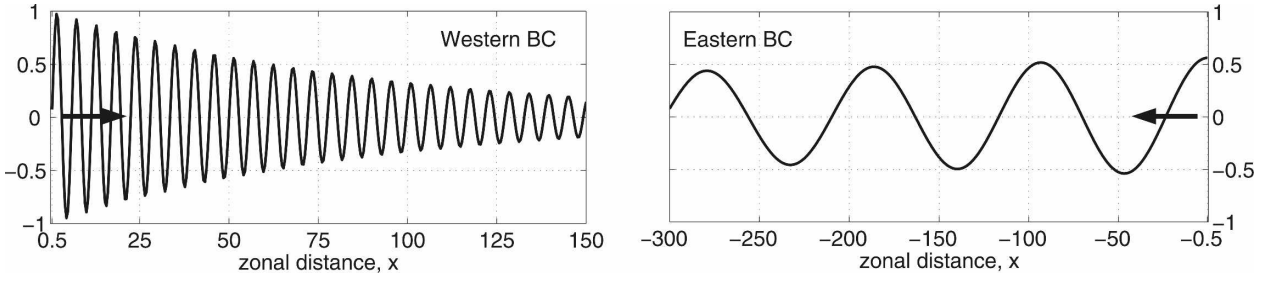

FIG. 4. Structure of a radiating wave (left) for the western and (right) eastern boundary currents for the barotropic case. Only the real part of the solution in the far-field $\phi(x)$ is plotted as a function of x. Western boundary current: $m = 0.348$, $c_r = 1.153$, $mc_i = 3.2 \times 10^{-3}$, $k = -1.140 + i0.011$. Eastern boundary current: $m = 0.348$, $c_r = 0.773$, $mc_i = 3.2 \times 10^{-3}$, $k = -0.068 - i0.001$.

0.080, its meridional phase speed is equal to minus one (i.e., it is opposite to the basic state current).

In addition to this mode, there are also other unstable eigenvalues (a representative is shown in Fig. 2 with a dotted–dashed gray line). Again, due to the trend of c_i to decrease to zero while c_r goes to 1 when the meridional wavenumber is increased, it is thought that these eigenvalues originate in their short-wave limit from the singular point $c = 1$, but because of the singularity, the limit cannot be reached numerically. The meridional phase speed for these modes decreases when m gets smaller and becomes $c_r = -1$ [i.e., opposite to the basic state current, when the modes stabilize (see Fig. 2a)]. Their growth rates are zero in both extremities and reach a maximum somewhere in between (see Fig. 2b). There are infinitely many eigenvalues (not only the one shown in the figures) with similar behavior, which reach their maximum growth rate at smaller and smaller values of m. A major difference from the western boundary current is that the accumulation point for these eigenvalues is $m = 0$ rather than m finite. In other words, there is no long meridional wave cutoff for the linear stability of an eastern boundary current.

Concerning the radiating nature of the instabilities, the logarithm of the ratio $|k_r|/|k_i|$, where k is the zonal wavenumber in the far field, is plotted in Fig. 3b as a function of the meridional wavenumber. Because for all eastern boundary current modes the meridional phase speed changes sign (it goes from being positive to -1 when m is decreased; see Fig. 2a), so does the real part of the zonal wavenumber in the far field. This corresponds to the minima of the dashed curves in Fig. 3b, where the far-field solution is characterized with $k_r \approx 0$. The solution has a radiating wave structure, as indicated by the positive values for $\log(|k_r|/|k_i|)$, to the left of the minimum (for all modes) and to the right of the minimum (for all but the leading unstable mode).

The long meridional wave end corresponds to a radiating instability, as for the western boundary current, because both k_i and the growth rate vanish. However, in this limit $k_r \approx 10^{-4}$ or smaller, depending on the mode, which leads to radiating waves with extremely long zonal wavelengths on the order of 10 000 current widths or more. Unlike for the western boundary current, there is an infinite number of eigenmodes with radiating wave structure toward the short meridional wave end. For all modes but the most unstable one, for values of the meridional wavenumber to the right of the minimum, the far-field solution is characterized with $|k_r| \gg |k_i|$ [positive values for $\log(|k_r|/|k_i|)$], while the growth rate is very weak, which is an indication of an eigenmode with horizontally radiating structure. In general, the smaller the meridional wavenumber, the stronger the growth rate and the greater the zonal wavelength of the radiated wave, with typical values between 20 and 2000 current widths.

An example of a far-field solution on the short meridional wave side of the minimum is shown in Fig. 4. The radiated wave has a meridional wavelength of $2\pi/m \approx 18$ current widths, a zonal wavelength of $2\pi/k_r \approx 90$ current widths, and an envelope decay scale of $1/k_i \approx 1000$ current widths. The solution has been chosen to have exactly the same growth rate as the solution for the western boundary discussed before. For the same growth rate, its longer envelope decay scale is due to the greater zonal group velocity: $c_g^x = -3.69$ for the eastern compared to $c_g^x = 0.29$ for the western boundary current, where the group velocity c_g^x is given in units of the current velocity V_*. This is consistent with the analysis in section 2b that the radiated waves from the eastern side are characterized with longer zonal wavelengths and a slower amplitude envelop decay due to the greater zonal group velocities than their western boundary counterpart.

As a final remark, in this barotropic model the only energy source for the growing instabilities is associated with the jump in the basic-state velocity. Thus, the radiating waves are considered the result of a Kelvin–Helmholtz-type instability of the flow.

3. The baroclinic case

In this section the problem of the linear stability of a purely baroclinic meridional current adjacent to a motionless far field is addressed using a two-layer QG model. The introduction of vertical structure leads to a model able to represent more physical processes. Specifically, the mean flow instabilities can be of the Kelvin–Helmholtz type, as in the barotropic case presented in section 2, or baroclinic instabilities because of the presence of vertical shear.

a. Formulation

For the two-layer case, the basic-state profile is again piecewise constant as sketched in Fig. 1, except that now the flow is chosen to be purely baroclinic:

$$V_{1,2} = \begin{cases} \pm\dfrac{Vs}{2}, & |x| < x_0 \\ 0, & |x| > x_0 \end{cases}. \tag{11}$$

Without loss of generality, the vertical shear V_S is chosen to be positive. The perturbation streamfunctions

for each layer $\psi_n(x, y, t)$ are once more decomposed into normal modes, $\psi_n(x, y, t) = \mathrm{Re}[\phi_n(x)\ e^{im(y-ct)}]$, where the amplitudes $\phi_n(x)$ satisfy the linearized quasi-geostrophic potential vorticity equation

$$(V_n - c)[\phi_n'' - m^2\phi_n + (-1)^n F_n(\phi_1 - \phi_2)] + \frac{\overline{Q}_{n,y}}{im}\phi_n' - \overline{Q}_{n,x}\phi_n = 0. \quad (12)$$

Here, $(\overline{Q}_{n,x}, \overline{Q}_{n,y})$ is the potential vorticity gradient of the basic state given by

$$\overline{Q}_{n,x} = \frac{d^2V_n}{dx^2} + (-1)^n F_n(V_1 - V_2), \overline{Q}_{n,y} = \beta. \quad (13)$$

All variables above are nondimensionalized, using as scales the vertical shear (V_S) and the Rossby deformation radius $L_d = \sqrt{2g'H_1H_2/f_0^2(H_1 + H_2)}$. The nondimensional parameters that appear in Eqs. (12) and (13) are the scaled planetary vorticity gradient $\beta = \beta_0 L_d^2/Vs$ and the parameters F_n, which are a function of the layer depths $F_n = 2H_1H_2/H_n(H_1 + H_2)$ with $F = F_1 + F_2 = 2$. Similar to the barotropic case, the jump conditions given by Eq. (5) as well as the no-normal flow condition on the solid wall are applied to each layer. The method of finding the eigenvalues is essentially the same except for a larger problem size. More details on the method of solution are given in the appendix.

The analysis from the barotropic case regarding how to identify the radiating instabilities is helpful for the two-layer model as well, although the situation is a little more complex. In the two-layer model, for a given choice of parameters β, F_1/F_2, and meridional wavenumber m, the solution in the far field is a superposition of two waves with zonal wavenumbers k_{bt} and k_{bc}, related to the frequency $\omega = cm$ by the barotropic and baroclinic Rossby wave dispersion relations, respectively:

$$cm = -\frac{\beta k_{\mathrm{bt}}}{k_{\mathrm{bt}}^2 + m^2}, \quad cm = -\frac{\beta k_{\mathrm{bc}}}{k_{\mathrm{bc}}^2 + m^2 + F}. \quad (14)$$

For both the barotropic and baroclinic parts of the far-field solution, an analysis similar to that in section 2b can be made. In particular, for an eigenvalue c satisfying the problem, there are two possible values for each of the wavenumbers k_{bt} and k_{bc} that have opposite-signed imaginary parts and zonal group velocities. The solution for a western boundary current has positive zonal group velocity, while for an eastern boundary current it has negative zonal group velocity, so that in both cases we have a vanishing perturbation at infinity. A solution qualifies as a radiating wave if in the limit of becoming neutrally stable the imaginary part of k_{bt} or of both k_{bt} and k_{bc} go to zero. The physical explanation behind this is the following: because the phase speed range of barotropic Rossby waves ($|c_r| < \beta/2m^2$) is wider than that of baroclinic Rossby waves ($|c_r| < \beta/2m\sqrt{m^2 + F}$), it may so happen that a solution has a radiating barotropic part but a nonradiating baroclinic part. If, however, the phase speed c lies within the range of the free baroclinic Rossby waves, then we have a solution that is a radiating wave and could have both barotropic and baroclinic components.

b. Energetics

In the two-layer QG model, the energy for the growing instabilities, be they radiating or not, can come from two sources—Kelvin–Helmholtz-type instability or baroclinic instability. To determine in what proportions these two sources contribute, one needs to consider the energy balance.

The energy equation can be derived by multiplying Eq. (12) by the complex conjugate amplitude ϕ_n^*, weighted by the layer depth $d_n = H_n/H$, and summing over the two layers. After several manipulations and using the fact that dV_n/dx is zero for the piecewise constant velocity profile used here, one can write the final result as

$$mc_iE = mF_0(V_1 - V_2)\mathrm{Im}(\phi_1\phi_2^*) + \frac{dS}{dx}, \quad (15)$$

where $E = F_0|\phi_1 - \phi_2|^2 + \Sigma_{n=1}^2 d_n(|\phi_n'|^2 + m^2|\phi_n|^2)$ is the total (potential plus kinetic) wave energy of the system with $F_0 = d_1F_1 = d_2F_2$. The quantity S is a flux term defined as

$$S = \sum_{n=1}^{2} \frac{\beta}{2} d_n|\phi_n|^2 - d_n\mathrm{Im}\left[m(V_n - c)\phi_n^*\frac{d\phi_n}{dx}\right]. \quad (16)$$

The energy flux S is zero at the solid wall and at infinity and undergoes a jump, proportional to the jump in the basic-state velocity, at the point where the velocity profile is discontinuous. Integrating Eq. (15) over the whole domain—from the wall to infinity for a western boundary current or from minus infinity to the wall for an eastern boundary current—leads to the following energy balance:

$$0 < \int mc_i E\, dx = \underbrace{\int_{-x_0}^{x_0} mF_0(V_1 - V_2)\mathrm{Im}(\phi_1\phi_2^*)\, dx}_{\mathrm{A}} + \underbrace{\Delta[S]}_{\mathrm{B}}. \quad (17)$$

For a linearly unstable, growing mode, the terms on the right-hand side have to sum to a positive number. Term A is the contribution from baroclinic instability where perturbations grow feeding on the potential energy of the basic-state flow, proportional to the vertical shear $(V_1 - V_2)$. Term B is the contribution from the flux term, which for $c_i \neq 0$ is nonzero only because there is a jump in the basic-state velocity profile at $x = +x_0$ for a western boundary current or at $x = -x_0$ for an eastern boundary current. This is interpreted as a Kelvin–Helmholtz type of instability that arises in the presence of discontinuous velocity profiles. In the barotropic model, the only source for growing perturbations is term B, while in the two-layer model terms A and B can combine in different ways and lead to growth.

c. Results

The baroclinic problem is characterized by three nondimensional parameters, which are β, F_1/F_2 or the ratio of the layer depths, and the nondimensional width of the current $2x_0/L_d$. In this section, results from calculations made with specific values of these parameters are shown. The layer depths are taken to be equal, which translates into $F_1 = F_2 = 1$, the width of the current is set to 10 deformation radii, and $\beta = \beta_0 L_d^2/V_S = 0.5$. As before, when solving the stability problem, the main objectives are to find the unstable eigenvalues, follow them as a function of the meridional wavenumber m, and determine whether they are radiating.

Before going into more details about the results, some general observations can be made that hold for both the western and eastern boundary current configurations. An examination of the problem solution shows that the unstable eigenvalues, if there are such, have real parts situated between $-0.5 < c_r < 0.5$, the nondimensional lower- and upper-layer basic-state velocity. In other words, the semicircle theorem seems to apply, although it cannot be proved for the meridional case (Walker and Pedlosky 2002). Furthermore, with the equal-layer depth assumption, the stability problem has the following symmetry property: if $c = c_r + ic_i$ is an eigenvalue of the problem, with corresponding eigenvectors $[\phi_1(x), \phi_2(x)]$, then $c = -c_r + ic_i$ is also an eigenvalue, with corresponding eigenvectors $[\phi_2^*(x), \phi_1^*(x)]$. Thus, there are two possibilities for the unstable eigenmodes: either they have a nonzero real phase speed, in which case they come in pairs $c = \pm c_r + ic_i$, or they have a zero real phase speed $c = 0 + ic_i$. The last ones are not of interest for radiating instabilities because $c_r = 0$ implies $\mathrm{Re}(k_{\mathrm{bt}}, k_{\mathrm{bc}}) = 0$ (i.e., no waves in the far field).

1) Western boundary current

In the short-wave end of the explored range of meridional wavenumbers, there is a single pair of unstable eigenvalues that asymptotes to $c = \pm 0.25 + i0.25$ as $m \to +\infty$ (black solid line in Figs. 5a,b). Again, as in the barotropic case, the lack of short-wave cutoff is related to the choice of piecewise constant basic-state profile with an infinitely thin region of horizontal shear. In addition to the leading pair, there are other pairs of unstable eigenvalues (two representatives are shown in Figs. 5a,b with gray solid lines). They originate from eigenvalues with zero real part (gray dashed lines in Figs. 5a,b) that collide and split into two unstable eigenvalues with nonzero real parts. When the meridional wavenumber is decreased, for all unstable pairs, the meridional phase speed c_r goes to ± 0.5, the upper- and lower-layer velocities, while the growth rate decreases. It was not possible to reach exactly the zero growth rate limit because the points $c = \pm 0.5$ are singular and it is very difficult to track eigenvalues in their vicinity. It is thought, however, that the modes stabilize when their meridional phase speed reaches the upper- or lower-layer velocity because of the decreasing trend for c_i. There is an infinite number of unstable pairs that originate from zero meridional phase speed modes at smaller and smaller meridional wavenumbers. Their accumulation point, however, is some finite critical wavenumber below which there are no more unstable modes. Thus, similar to the barotropic western boundary current, there is a long meridional wave cutoff for the linear stability of a purely baroclinic western boundary current.

Concerning the radiating nature of the instabilities, the logarithm of the ratios $|k_r^{\mathrm{bt}}|/|k_i^{\mathrm{bt}}|$ and $|k_r^{\mathrm{bc}}|/|k_i^{\mathrm{bc}}|$, where k^{bt} and k^{bc} are the zonal wavenumbers for the barotropic and baroclinic parts of the far-field solution, are plotted as a function of the meridional wavenumber in Figs. 5c,d, respectively. These plots show only the modes with nonzero meridional phase speed, which are the only ones that can possibly have wave structure in the far field. Although it was not possible to reach exactly the limit $c_i = 0$, there is an indication that for both

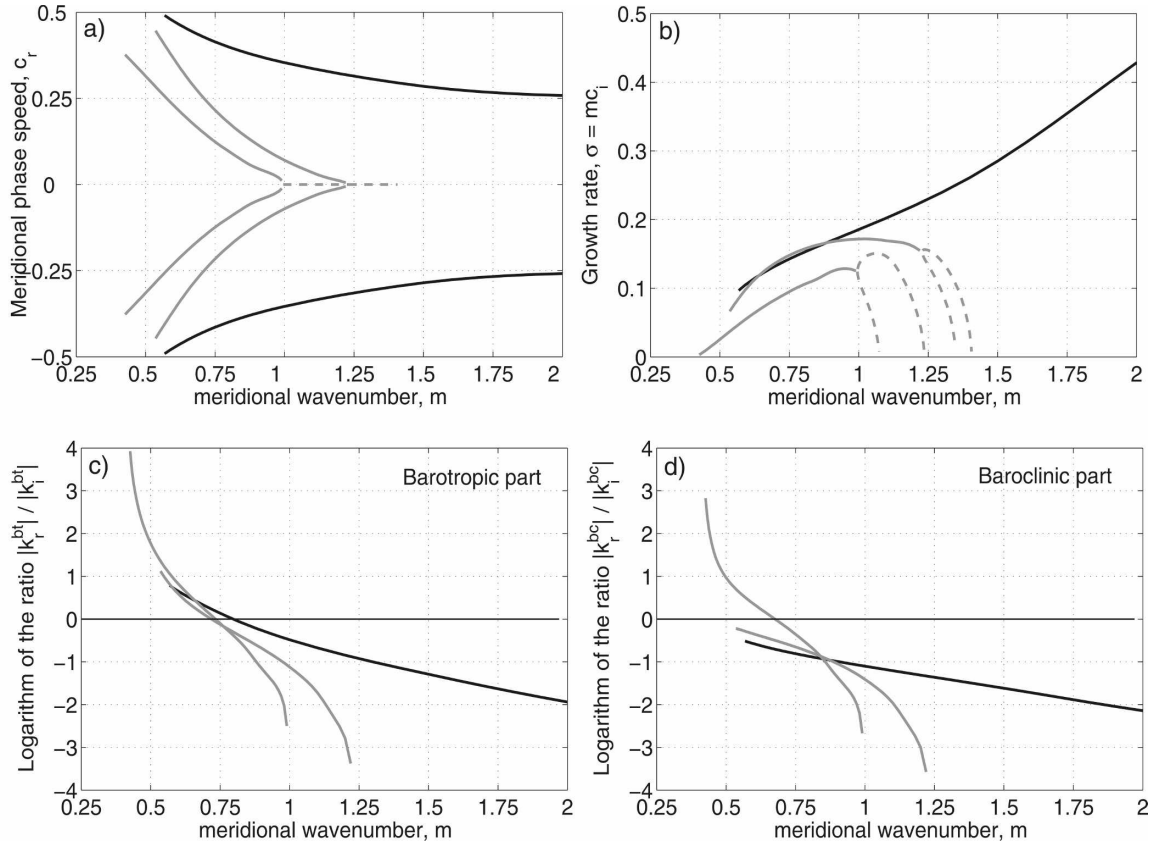

FIG. 5. For the baroclinic western boundary current configuration with $\beta = 0.5$ and $F_1 = F_2 = 1$, (a) meridional phase speed, (b) growth rate and logarithm of the ratio $|k_r|/|k_i|$ for the (c) barotropic and (d) baroclinic parts of the far-field solution as a function of the meridional wavenumber. The first 10 unstable eigenvalues are shown using black solid lines for the leading unstable pair, gray solid lines for the next unstable pairs, and gray dashed lines for the eigenvalues with $c_r = 0$ (nonradiating).

the barotropic and the baroclinic parts of the solution the long-wave end of the explored range of meridional wavenumbers is radiating because $|k_r| \gg |k_i|$ while $mc_i \to 0$. This is especially true for the pairs of modes that destabilize at smaller meridional wavenumbers but not so much for the leading pair of unstable modes. Note that although the eigenmodes with radiating structure in the far field are found toward the long-wave end of the explored range of meridional wavenumbers ($m < 0.75$), the corresponding meridional wavelength of the disturbances is actually not so large—it is only a couple of deformation radii.

Finally, it is worth noticing that the stability picture, where pairs of unstable modes originate from modes with zero meridional phase speed and stabilize when they reach the basic-state velocities, is very similar to what is occurring in a meridional flow confined in a channel: the configuration studied in detail in Walker and Pedlosky (2002) and Pedlosky (2002). The reason for the instability in this case is identified as being the destabilization of Rossby normal modes by the vertical shear. The resemblance to the channel case suggests that despite the addition of a motionless far field on one side of the meridional flow, the same physical mechanism for the instability may be in play.

2) EASTERN BOUNDARY CURRENT

The eigenvalue analysis of an eastern boundary current is qualitatively similar for the most part to the western counterpart. In the short-wave end of the explored range of meridional wavenumbers, there is a single unstable pair that asymptotes to $c = \pm 0.25 + i0.25$ (black solid line in Figs. 6a,b). Additional pairs of unstable eigenvalues appear from the splitting of zero meridional phase speed eigenvalues (two representatives are shown in Figs. 6a,b with gray solid line). When the wavenumber is decreased, the meridional phase speed for all unstable pairs goes toward $c_r = \pm 0.5$, the upper and lower basic-state velocities, where the modes are thought to stabilize (although the exact zero growth rate limit cannot be reached computationally). This

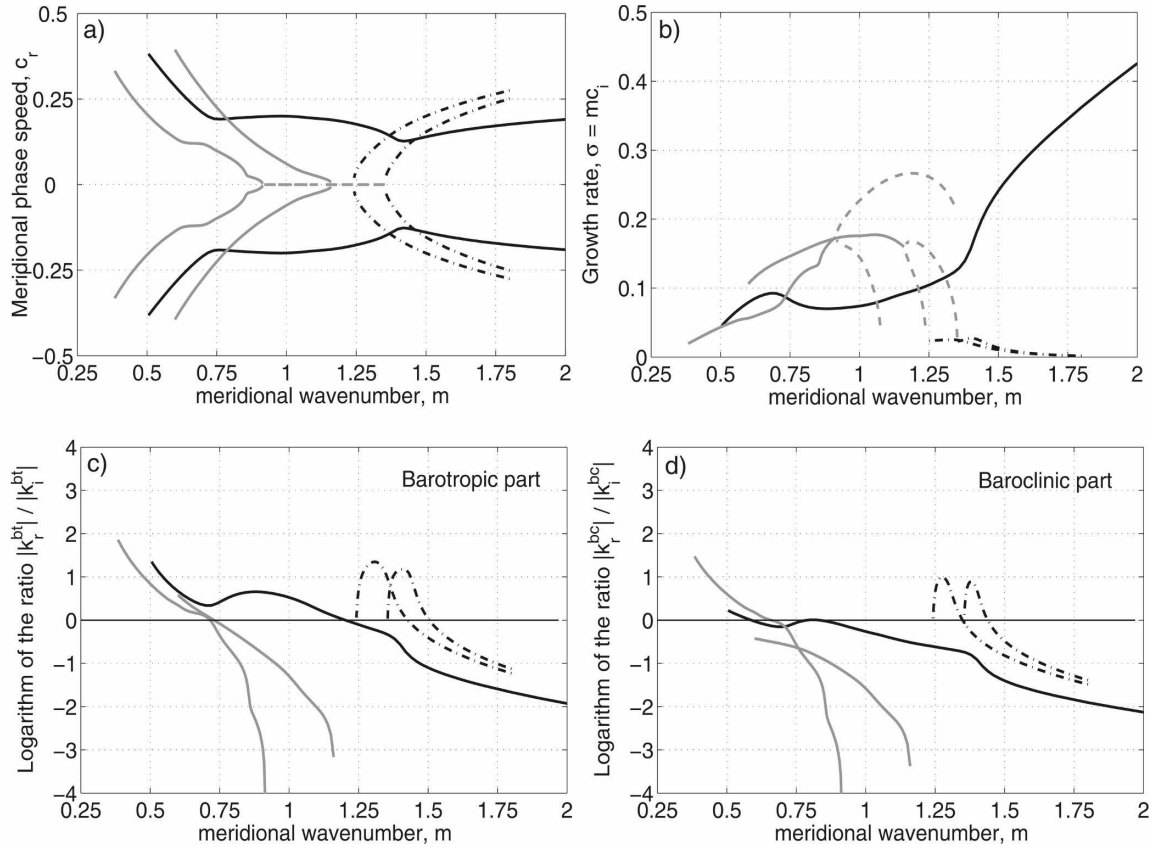

FIG. 6. As in Fig. 5, but for the baroclinic eastern boundary current configuration. The first 14 unstable eigenvalues are shown using black solid lines for the leading unstable pair, gray solid lines for the next unstable pairs, gray dashed lines for the eigenvalues with $c_r = 0$ (nonradiating), and black dotted–dashed lines for the weakly unstable pairs, present in the eastern case only.

again bears similarities to the instability of a meridional channel flow studied in Walker and Pedlosky (2002).

There are also some differences from the western case. First, there is a range of meridional wavenumbers over which the additional pairs are the most unstable modes with growth rates almost twice as large as the leading pair. Another difference is that there is a whole group of weakly unstable eigenmodes, not present in the western case (two such pairs, the most unstable ones, are shown in Figs. 6a,b with black dotted–dashed lines). These weakly unstable modes are characterized with meridional phase speeds that decrease from $c_r = \pm 0.5$ toward $c_r = 0$ when the meridional wavenumber is decreased. These modes seem to be at the origin of the zero meridional phase speed modes (gray dashed line in Figs. 6a,b)—when a pair of weakly unstable modes reaches $c_r = 0$, they collide and a single unstable eigenvalue with $c_r = 0$ appears. As we will see later, the energetics for these weakly unstable modes is also different, which suggests that a different mechanism for the instability is at play. Finally, similar to the barotropic case, the accumulation point for the infinite number of unstable modes is $m = 0$, so that there is no long meridional wave cutoff for the linear stability of a purely baroclinic eastern boundary current.

Concerning the presence of radiating waves, the logarithm of the ratios $|k_r^{bt}|/|k_i^{bt}|$ and $|k_r^{bc}|/|k_i^{bc}|$ are plotted for all nonzero meridional phase speed modes in Figs. 6c,d, respectively. In a comparable way to the western case, it is the long-wave end of the explored range of meridional wavenumbers that seems to be radiating, because $|k_r| \gg |k_i|$ while $mc_i \to 0$ for both the barotropic and the baroclinic part. Exceptions are the weak growth rate eigenmodes that exist in the eastern case only. For these modes, neither their short- nor their long-wave limit is radiating, even though the eigenvectors have a radiating wave structure in the far field [positive values for log $(|k_r^{bt}|/|k_i^{bt}|)$ and log $(|k_r^{bc}|/|k_i^{bc}|)$] for some range of meridional wavenumbers in between.

Examples of radiating wave solutions for the western and eastern configurations are shown in Fig. 7. First, as could be expected, waves from the western side are characterized by smaller zonal wavelengths and faster

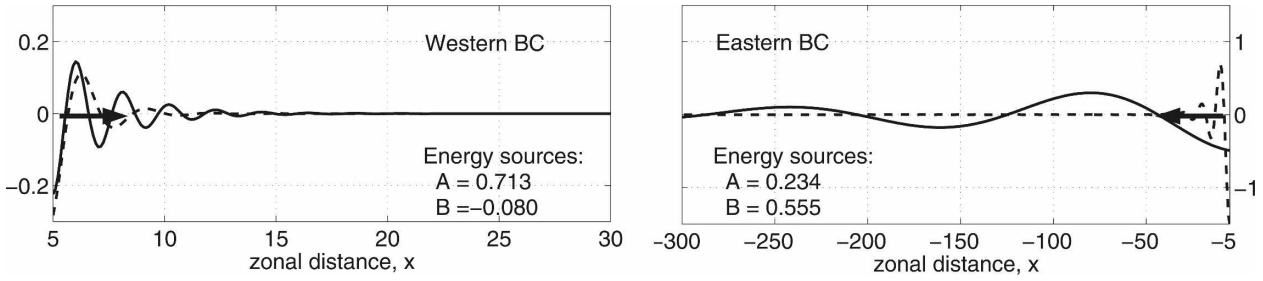

FIG. 7. Structure of a radiating wave for the (left) western and (right) eastern boundary currents for the baroclinic case. Only the real part of the solution in the far field $\phi(x)$ is plotted as a function of x. Solid line is the barotropic part; dashed line is the baroclinic part of the solution. Western boundary current: $m = 0.486$, $c_r = -0.326$, $mc_i = 2.1 \times 10^{-2}$, $k_{\rm bt} = 3.021 + i0.419$, $k_{\rm bc} = 2.168 + i0.715$. Eastern boundary current: $m = 0.390$, $c_r = -0.324$, $i = 2.1 \times 10^{-2}$, $k_{\rm bt} = 0.039 - i0.007$, $k_{\rm bc} = 0.630 - i0.154$.

amplitude decay away from the current compared to the eastern case. For the western boundary current solution, the radiated barotropic and baroclinic waves have comparable zonal wavelengths on the order of two to three deformation radii and an envelope decay scale on the order of one to two deformation radii. For the eastern boundary current solution, the baroclinic wave is of zonal length $2\pi/k_r^{\rm bc} \approx 10$ deformation radii, while the barotropic wave is much longer: $2\pi/k_r^{\rm bt} \approx 160$ deformation radii. Because the envelope decay scale for the baroclinic part is much shorter compared to that for the barotropic part however (6 compared to 140 deformation radii), the solution far away from the current is predominantly barotropic. Second, a peculiarity about the horizontal structure of the far-field solution is brought to light if one looks at the meridional wavelength of the radiated waves. For both the eastern and the western case solutions, the meridional wavelength of the waves is on the order of $2\pi/m \approx 15$ deformation radii, while their zonal wavelengths are significantly different. We find that waves radiated from the eastern side tend to be asymmetric, in the sense that they are much longer in the zonal direction than in the meridional. This leads to a velocity field with a zonal component much larger than the meridional component, which would cause the radiating waves to appear, as they propagate in the far field, more like zonal jets than localized wave packets or eddies.

3) ENERGETICS

An inspection of the energy balance for the unstable eigenmodes can give some insight into the processes responsible for the instability. For the leading pair (black solid lines in Figs. 5, 6), especially in the short-wave end of the explored range of meridional wavenumbers, the most important energy source is term B, or Kelvin–Helmholtz-type instability related to the jump in the basic-state velocity profile. This holds for both the western and eastern boundary current setups and supports the idea that the lack of short-wave cutoff is due to the choice of discontinuous velocity profile. Concerning the other pairs of unstable eigenmodes (solid gray lines in Figs. 5, 6), there is a significant difference between the western and eastern configurations. For the western case, the dominant energy source is term A, or the baroclinic instability, while term B, related to the jump in the basic-state velocity, is negligible (see the western solution in Fig. 7). For the eastern case, both terms A and B are positive and contribute in comparable amounts (see the eastern solution in Fig. 7). The fact that in both configurations the baroclinic conversion term A is important for the pairs of eigenmodes originating from splitting of modes with zero real part eigenvalues further supports the connection to the meridional channel flow instability due to the destabilization of Rossby normal modes by the vertical shear, as discussed in Walker and Pedlosky (2002) and Pedlosky (2002). Finally, for the weak growth rate eigenmodes that exist only in the eastern configuration (black dotted–dashed lines in Fig. 6), the baroclinic conversion term A is negative, while term B related to the jump in the mean velocity is positive and slightly bigger in magnitude so that we have a growth overall. This is a different energy balance compared to the other unstable modes, which suggests a different instability mechanism.

One can also use the energy balance to get some indications about the potential effect of the radiating modes on the current. The solutions shown in Fig. 7 have been plotted with a mode amplitude chosen so that the perturbation velocities within the boundary current region are of the same order as the basic-state current itself. Although one would not expect a linear stability analysis to hold at such large amplitudes, this is a reasonable assumption for regions of unstable oceanic currents, where the meanders lead to perturbations of

the same order as the mean, and is done to get realistic magnitude for the energy fluxes. Given the total energy contained in the basic state $E = \int_{-x_0}^{x_0}(V_1^2 + V_2^2 + V_s^2x^2)/2\, dx$, one can then use the fluxes A and B to find the time needed to utilize all of the basic-state energy toward growing perturbations. Note that in the framework of the linear stability analysis performed here, the flow is not actually evolving in time. The basic-state velocity profile is constantly supplied with energy from some external forcing (wind, e.g.) so that it is fixed in time. The depletion time scale defined above is thus only a hypothetical quantity helpful in judging the effect of the radiating modes on the current; no actual time evolution computations are performed.

The depletion time scales found using the fluxes for the specific solutions in Fig. 7 are on the order of 50–70 time units. Those are comparable to the growth time scale, which is $1/mc_i \approx 48$ time units. If the nondimensional parameter $\beta = 0.5$ is representative of a current with deformation radius $L_d = 60$ km and vertical shear $V_S = 15$ cm s^{-1}, then the depletion times are on the annual scale, which implies a minor effect on the current.

4. Discussion and conclusions

In this paper we have performed a linear stability analysis of a meridional boundary current adjacent to a motionless far field. The current is idealized as a piecewise constant linear profile as in Fantini and Tung (1987), which allows the stability problem to be reduced to a nonlinear algebraic equation that can be solved numerically. We are interested in a special type of instability of this system. When the phase speed and wavenumber of the disturbances within the unstable region are such that they match those of the freely propagating Rossby waves in the far field, temporally growing radiating waves with amplitude envelopes that decay slowly with distance from the source may appear. These are called radiating instabilities. The existence of radiating instabilities is of interest because even if the radiating modes are not the most unstable modes, they are the only ones that reach the neutral far field. By transporting perturbation energy away, they have the ability to affect the circulation far from the locally unstable region where the perturbations are generated.

We have considered two different cases of a basic-state flow: a purely barotropic and a purely baroclinic meridional velocity profile, because it was determined that the stability of a more general flow, which is still piecewise constant but has both barotropic and baroclinic components, is a mix of the behavior of the purely barotropic and purely baroclinic cases.

The first major conclusion of this paper is that unlike zonal currents, for which special circumstances are needed, unstable meridional currents are generally characterized by eigenmodes that have a horizontally radiating structure. The radiating modes are not necessarily the most unstable ones, but there are usually several of them for a given set of parameters. In the two-layer case, the radiating solutions have both barotropic and baroclinic components.

A second major conclusion of this paper concerns the differences in the stability properties of western and eastern meridional boundary currents. For instance, it was found that western boundary currents are linearly stable to perturbations with meridional wavenumbers below some critical value, while there is no such long meridional wave cutoff for the linear stability of eastern boundary currents. What is at the base of these differences is the requirement that the zonal group velocity of the radiated waves be away from the locally unstable region. Consequently, western boundary currents radiate short Rossby waves ($k_r > m$), which have a small eastward group velocity and a rapidly decaying amplitude envelope away from the current. Eastern boundary currents, on the other hand, radiate long Rossby waves ($k_r < m$), which have a large westward group velocity and a slowly decaying amplitude envelope away from the current. It was determined that not only do radiating waves from the eastern side penetrate farther into the far-field region but there is a greater number of them and they can be found over a wider range of meridional wavenumbers. Another particularity of the eastern boundary current radiating waves is that they tend to have an asymmetrical horizontal structure with a zonal wavelength several times larger than the meridional wavelength. This leads to a velocity field with a zonal component much larger than the meridional component, which would cause the radiating waves to appear, as they propagate in the far field, more like zonal jets than localized wave packets or eddies. Circulation in the form of multiple zonal jets has been observed in the real ocean (Maximenko et al. 2005). In particular, the eastern parts of all basins at midlatitudes contain signatures of steady alternating jets with a meridional scale on the order of 200–300 km and extending zonally for thousands of kilometers (Maximenko and Niiler 2006). The origin of these jets is not yet fully understood. The present study brings the possibility that the observed zonal jets may be related to radiating instabilities of eastern boundary currents.

We have also looked at the energy balance, which gives some insight into the sources for the instabilities. In the barotropic model, the only energy source is a Kelvin–Helmholtz type of instability due to the discon-

tinuous velocity profile. In the two-layer case, a second possible energy source is baroclinic instability because of the presence of vertical shear. There are some differences between the energy balance for the western and eastern cases. However, the fact that the baroclinic conversion term contributes significantly to the energy balance for all unstable modes except the leading one, for both eastern and western boundary currents, suggests a connection to the meridional channel flow instability studied in Walker and Pedlosky (2002).

As a final word, although the model used in this study is very idealized, it leads to some interesting conclusions concerning the differences between eastern and western meridional boundary currents and the characteristics of the radiating waves, all of which are worth pursuing using more realistic models.

Acknowledgments. This work was supported by the National Science Foundation through Grants OCE-0423975 (MS, HH) and OCE-9901654 (JP). HH would like to thank her thesis committee as well as the MIT–WHOI Joint Program for partial financial support. We wish to also thank two anonymous reviewers for helping improve the clarity of the presentation.

APPENDIX

Method of Solution

a. The barotropic case

The linear stability Eq. (3) to be solved is a constant coefficient ODE because the basic-state velocity is constant in the two regions, boundary current $|x| < x_0$ and far-field $|x| > x_0$. The solution in the boundary current region, where V is a nonzero constant, is

$$\phi^{\text{in}}(x) = \sum_{j=1}^{2} B_j e^{ik_j x}, \tag{A1}$$

where the zonal wavenumbers k_j are the two roots of the second-order polynomial

$$k^2(V - c) - \frac{\beta}{m}k + m^2(V - c) = 0.$$

The solution in the far-field region is a particular case with $V = 0$ of the boundary current solution. The two roots of the second-order polynomial in this case are

$$k_{\text{bt}}^{\pm} = \frac{\beta}{2cm}\left(-1 \pm \sqrt{1 - \frac{4c^2m^4}{\beta^2}}\right).$$

Only one of the zonal wavenumbers $k_{\text{bt}}^{\pm}$ is physically consistent for the far-field solution. The minus sign corresponds to barotropic Rossby waves that have a positive group velocity—this is the choice for a *western* boundary current. The plus sign corresponds to barotropic Rossby waves that have a negative group velocity—this is the choice for an *eastern* boundary. Therefore, the solution in the far-field region, for the western and eastern boundary currents, respectively, is

$$\phi^{\text{out}}(x) = B_3 e^{ik_{\text{bt}}^{\mp}(x \mp x_0)}. \tag{A2}$$

For a given parameter β and a meridional wavenumber m, the constants B_j and the eigenvalue(s) c, which appear in the solutions (A1) and (A2) through the expressions for the zonal wavenumbers, are found by imposing the no-normal flow condition at the wall and the jump conditions (5) on the side with discontinuous velocity. These conditions translate into the following set of equations, for the western and eastern cases, respectively:

$$\text{at } x = \mp x_0 : \phi^{\text{in}} = 0, \tag{A3}$$

$$\text{at } x = \pm x_0 : \frac{\phi^{\text{in}}}{V - c} = \frac{\phi^{\text{out}}}{-c}, \tag{A4}$$

$$\text{at } x = \pm x_0 : (V - c)\frac{d\phi^{\text{in}}}{dx} + \frac{\beta}{im}\phi^{\text{in}} = -c\frac{d\phi^{\text{out}}}{dx} + \frac{\beta}{im}\phi^{\text{out}}. \tag{A5}$$

It is straightforward to see that after using the expressions (A1) and (A2), the equations above lead to a homogeneous 3×3 system for the unknown constants $(B_j)_{j=1}^{3}$. The eigenvalues c are those values for c that make the determinant of the homogeneous system zero, so that there is a nontrivial solution for the constants B_j. Once the eigenvalue(s) c are found, if there are such, the solution in all regions can be reconstructed.

b. The baroclinic case

The linear stability problem (12) is solved following the same procedure, except that now we are dealing with two layers. The solution in the boundary current region, where V_n are nonzero constants, is

$$\phi_1^{\text{in}}(x) = \sum_{j=1}^{4} B_j e^{ik_j x}, \tag{A6}$$

$$\phi_2^{\text{in}}(x) = \sum_{j=1}^{4} B_j \Gamma_j e^{ik_j x},$$

where

$$\Gamma_j = \frac{k_j^2}{F_1} + \frac{\beta k_j}{m(c - V_1)F_1} + \frac{m^2}{F_1} + \frac{c - V_2}{c - V_1},$$

and the zonal wavenumbers k_j are the four roots of the fourth-order polynomial

$$\alpha_4 k^4 + \alpha_3 k^3 + \alpha_2 k^2 + \alpha_1 k + \alpha_0 = 0,$$

with

$$\alpha_4 = (c - V_1)(c - V_2),$$
$$\alpha_3 = (2c - V_1 - V_2),$$
$$\alpha_2 = \left(\frac{\beta}{m}\right)^2 + (2m^2 + F)\alpha_4 + (V_1 - V_2)\gamma,$$
$$\alpha_1 = \frac{\beta}{m}(m^2\alpha_3 + \gamma),$$
$$\alpha_0 = m^2[(m^2 + F)\alpha_4 + (V_1 - V_2)\gamma],$$
$$\gamma = F_1(c - V_2) - F_2(c - V_1).$$

In the far-field region, where $V_n = 0$, the fourth-order polynomial reduces to the barotropic and baroclinic Rossby dispersion relations, so that the four roots k_j become

$$k_{\mathrm{bt}}^{\pm} = \frac{\beta}{2cm}\left(-1 \pm \sqrt{1 - \frac{4c^2m^4}{\beta^2}}\right),$$
$$k_{\mathrm{bc}}^{\pm} = \frac{\beta}{2cm}\left[-1 \pm \sqrt{1 - \frac{4c^2m^2(m^2 + F)}{\beta^2}}\right].$$

Once more, only one of the signs in the expressions above corresponds to barotropic and baroclinic Rossby waves with zonal group velocity in the right direction. Thus, the solution in the far-field region, for the western and eastern cases, respectively, is

$$\phi_1^{\mathrm{out}}(x) = \frac{1}{2}B_5 e^{ik_{\mathrm{bt}}^{\mp}(x \mp x_0)} + \frac{F_1}{F}B_6 e^{ik_{\mathrm{bc}}^{\mp}(x \mp x_0)}, \quad \text{(A7)}$$
$$\phi_2^{\mathrm{out}}(x) = \frac{1}{2}B_5 e^{ik_{\mathrm{bt}}^{\mp}(x \mp x_0)} - \frac{F_2}{F}B_6 e^{ik_{\mathrm{bc}}^{\mp}(x \mp x_0)}.$$

Applying the no-normal flow condition at the wall and the jump conditions (5) for each layer translates into the following set of equations:

$$\text{at } x = \mp x_0 : \phi_n^{\mathrm{in}} = 0, \; n = 1, 2, \quad \text{(A8)}$$
$$\text{at } x = \pm x_0 : \frac{\phi_n^{\mathrm{in}}}{V_n - c} = \frac{\phi_n^{\mathrm{out}}}{-c}, \quad n = 1, 2, \quad \text{(A9)}$$
$$\text{at } x = \pm x_0 : (V_n - c)\frac{d\phi_n^{\mathrm{in}}}{dx} + \frac{\beta}{im}\phi_n^{\mathrm{in}} = -c\frac{d\phi_n^{\mathrm{out}}}{dx} + \frac{\beta}{im}\phi_n^{\mathrm{out}}, \quad n = 1, 2. \quad \text{(A10)}$$

This leads, after using the expressions (A6) and (A7), to a homogeneous 6×6 system for the unknown constants $(B_j)_{j=1}^6$. Again, the eigenvalues c are those values for c that make the determinant of the homogeneous system zero, so that there is a nontrivial solution for the constants B_j. Once the eigenvalue(s) c is found, if there is such, the solution in all regions and layers can be reconstructed.

REFERENCES

Fantini, M., and K.-K. Tung, 1987: On radiating waves generated from barotropic shear instability of a western boundary current. *J. Phys. Oceanogr.,* **17,** 1304–1308.

Kamenkovich, I., and J. Pedlosky, 1996: Radiating instabilities of nonzonal ocean currents. *J. Phys. Oceanogr.,* **26,** 622–643.

Maximenko, N., and P. Niiler, 2006: Mean surface circulation of the global ocean inferred from satellite altimeter and drifter data. *Proc. Symp. on 15 Years of Progress in Radar Altimetry,* Venice, Italy, European Space Agency, SP-614. [Available online at http://earth.esa.int/cgi-bin/confalt15y.pl?abstract=780.]

——, B. Bang, and H. Sasaki, 2005: Observational evidence of alternating zonal jets in the world ocean. *Geophys. Res. Lett.,* **32,** L12607, doi:10.1029/2005GL022728.

Pedlosky, J., 2002: The destabilization of Rossby normal modes by meridional baroclinic shear. *J. Phys. Oceanogr.,* **32,** 2418–2423.

Talley, L. D., 1983: Radiating instabilities of thin baroclinic jets. *J. Phys. Oceanogr.,* **13,** 2161–2181.

Walker, A., and J. Pedlosky, 2002: Instability of meridional baroclinic currents. *J. Phys. Oceanogr.,* **32,** 1075–1093.